JOURNAL OF
ENVIRONMENTAL HYDROLOGY
The Electronic Journal of the International Association for Environmental Hydrology
On the World Wide Web at http://www.hydroweb.com
VOLUME 21 2013

ESTIMATION OF ACTUAL EVAPOTRANSPIRATION USING SURFACE ENERGY BALANCE ALGORITHMS FOR LAND MODEL: A CASE STUDY IN SAN JOAQUIN VALLEY, CALIFORNIA

Sagarika Roy [1]
Duke Ophori [1]
Shawn Kefauver [2]

[1] Montclair State University, Montclair, New Jersey
[2] University of California, Davis, California

Almond is an important cash crop in semi-arid southern San Joaquin Valley, California. Estimating almond water use is an important research objective in the arid area of Paramount farm. A Surface Energy Balance Algorithm for Land (SEBAL) model spatially estimates actual evapotranspiration (ETa) in the southern San Joaquin Valley in California from available MASTER airborne data. The objectives of the study are: (1) to study the spatial distribution property of canopy surface temperature (Tc), Normalized Difference Vegetation Index (NDVI), and ETa over the San Joaquin Valley, (2) estimate ETa of almond class on pixel-by-pixel basis in the Central Valley, California, and (3) to compare ETa obtained from SEBAL model with Penman- Monteith method. The results show that the regression between ETa, and Tc show negative (-) correlation. The correlation coefficient of ETa from remote sensing with Penman Monteith was 0.85 with bias of 0.77 mm and mean percentage difference is 0.10%. These results indicate that a combination of MASTER data with surface meteorological data could provide an efficient tool for the estimation of regional actual ET used for water resources, irrigation scheduling and management.

INTRODUCTION

Almond is an important cash crop in semiarid southern San Joaquin Valley, California. However, water use by almond trees is greater than most row crops. Estimation of actual evapotranspiration (ETa) is widely used to recognize the quantity of water applied as "intended" or not. Unfortunately, ground measurement of evapotranspiration (ET) is a very time consuming and cannot obtain accurate spatial ET estimation. Therefore, the complexity involved with the estimation of ET manually resulted in development of various spatial methods using remote sensing over the period of time (Allen et al., 1998). During the last two to three decades, significant progress was made to estimate ETa using satellite remote sensing (Engman and Gurney, 1992; Kustas and Norman, 1996; Bastiaanssen et al., 1998 and Kustas et al., 2003; Courault et al., 2003). These approaches provide a powerful means to compute ETa from the scale of an individual pixel right up to an entire raster image. There are two main methods in remote sensing for estimation of ET : direct and indirect. Direct method use thermal infrared data (TIR) and energy budget equations. Indirect method use Soil-Atmosphere Transfer models. These methods use different wavelength data to obtain ground surface characteristics such as albedo, emissivity, and leaf area index (Courault et al., 2003). In this study, direct measurement of ET using the Surface Energy Balance Algorithm for Land (SEBAL) applied in the agricultural land of southern San Joaquin Valley in California. SEBAL is one of the residual method of energy balance, developed by Bastiaanssen et al. (1998). It combines empirical and physical parameterization. The inputs include local weather data (mainly wind speed) and satellite data (radiance). From the input data, the net solar radiation, NDVI, albedo, roughness length, and G (soil heat flux) are calculated. The objective of this study is to (1) investigate the spatial distribution property of land surface temperature (Ls), Normalized Difference Vegetation Index (NDVI), and ETa over the San Joaquin Valley. (2) Estimate actual evapotranspiration of the almond class on a pixel-by-pixel basis in the Central Valley, California using Image classification and Mask, (3) to compare actual evapotranspiration obtained from SEBAL model with reference evapotranspiration (ETo) using Penman Monteith (PM) method obtained from California Irrigation Management Information System (CIMIS) station.

MATERIALS AND METHOD

Study area

The 402 km^2 Paramount Farm is located at the Lost Hill of Kern County in southern San Joaquin Valley of California (35^{o}30'N, 119^{o}39'W) (Figure 1). The total annual rainfall in 2009 drought year of the farm was 98.5 mm. The valley occupies two-thirds of the southern Central Valley in California. San Joaquin River flows in the northern part of the San Joaquin Valley and drains to the San Francisco Bay. About 4 percent of the basin area is urban. About 4 percent of the basin area is urban. Most of the basin's population is focused on agricultural activities. Southern San Joaquin is the world's largest supplier of almonds with more than 4,000 acres of almond orchards. Geographically, the southern part of the San Joaquin Valley is the Tulare Basin, bordered by the Sierra Nevada on the east, the Tehachapi Mountains on the south, and the Coast Ranges on the west. The northern extent corresponds to the Kings River. Significant geographic features include the Tulare Lake Basin and the Kettleman Hills. The main land use is agriculture. The study area is irrigated under CVP, which supplies water from the Sacramento-San Joaquin river system. Therefore, the quantification of ET is necessary to understand the crop water use.

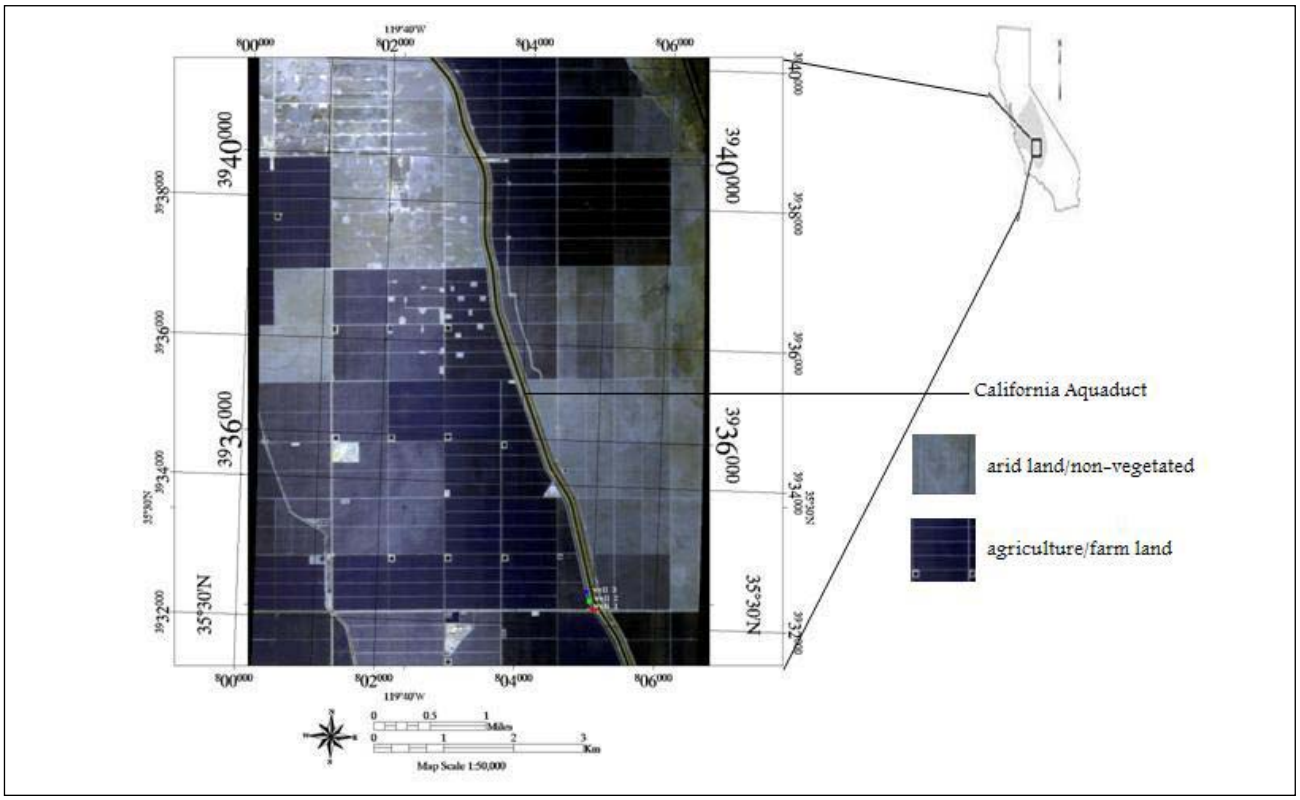

Figure 1. Remotely sensed false color composite (Band 1, Band 2 and Band 6) of MASTER image showing Paramount farm in Southern San Joaquin Valley, California. Blocks shows reflectances of various types of crops in dark tone. Bright tone shows reflectances of non-vegetated/arid areas (Land cover classification of this image shown in Figure 2-3a).

Data

An airborne image was obtained from MASTER (MODIS/ASTER) sensor. This simulator has the characteristics of both the EOS Terra Advanced Spaceborne Thermal Emission Reflection Radiometer (ASTER) and Moderate Resolution Imaging Spectroradiometer (MODIS) sensors (Hook et al., 2000). This sensor has 50 spectral bands in four spectral regions (visible through thermal infrared) with greater than 10 m spatial resolution. An image was taken on July 24, 2009. Field data was also available for calibrating land surface heat fluxes in the study area. SEBAL model was applied to level 1 B dataset of visible, near infrared and thermal infrared radiation channels of airborne MASTER instrument on board the NASA DC-8 aircraft. Meteorological data such as incoming solar radiation, relative humidity, air temperature, and wind speed are available from the California Irrigation Management Information System (CIMIS) located in Belridge, California (station no. 146). CIMIS is a program governed by the Department of Water Resources (DWR) in California. DWR manages a network of 120 weather stations to collect, store and process weather data. These data are useful for irrigator to manage water resources efficiently.

SEBAL Model Description

The SEBAL model does not only calculate a entire radiation and energy balance, but also computes resistances for momentum, heat , and water vapor transport for each pixel (Bastiaanssen et al., 1998 and Bastiaanssen et al., 2000). The main input for SEBAL consists of spectral radiance in the visible, near infrared, and thermal infrared part of the electromagnetic spectrum. This model requires the weather data parameters (wind speed, humidity, solar radiation, air temperature) and

remote sensing (satellite or airborne) images. When considering instantaneous conditions, the energy balance for a land surface is given as:

$$Rn = G_0 + H + LE \ (W\ m^{-2}) \quad (1)$$

where Rn is the net radiation [W m^{-2}], G_0 is the soil heat flux [W m^{-2}], H is the sensible heat flux [W m^{-2}] and LE is the latent heat flux [W m^{-2}], which is equal to AET. Other factors affecting the energy balance such as heat stored by the vegetation and photosynthesis are usually neglected , because they are considered to be a small fraction of net radiation when compared with the other four components when compared with the other four components (Allen et al., 1998). Equation (1) can also be expressed in terms of latent heat flux.

$$LE = EF\ (Rn_{24} - G_0)\ (W\ m^{-2}) \quad (2)$$

where EF is the evaporative fraction. The instantaneous evaporative fraction (EF), and the daily averaged net radiation, Rn_{24} is used to calculate evaporation. The EF is defined as the ratio of evapotranspiration to the available energy.

$$\frac{LE}{H + LE}\ (W\ m^{-2}) \quad (3)$$

The EF is supposed to be constant during daytime hours, even though H and LE differ considerably (Crago, 1996). When the atmospheric moisture and soil moisture are in equilibrium, then the EF expresses the ratio of the actual to the crop evaporative demand. The incoming solar radiation is measured using a pyranometer. The instantaneous net radiation (Rn) was calculated between (↓) and outgoing fluxes (↑) of shortwave R_S and long wave R_L radiation. Negative fluxes are considered to be those leaving the surface and positive for those incoming to the surface. Further, to solve for Equation 2, the values of Rn, EF and G_0 are computed using the surface radiation balance equation:

$$Rn = R_S\downarrow - aR_S\downarrow + R_L\downarrow - R_L\downarrow - (1 - \varepsilon_o)R_L\downarrow \ \ (W\ m^{-2}) \quad (4)$$

where $R_S\downarrow$ is the incoming shortwave radiation (W/m^2), a is the surface albedo (dimensionless) ,RL↓ is the incoming long wave radiation (W/m^2), $R_L\downarrow$ is the outgoing long wave radiation (W/m^2), and ε_o is the surface thermal emissivity (dimensionless)

The amount of energy absorbed to sustain crop evaporation rate describes the latent heat flux. The surface temperature, vegetation index and surface albedo are derived from remote sensing measurements, and used together to solve for Rn, G_0 and H. Surface emissivity is obtained according to the relationship proposed by Van de Griend and Owe, 1993

$$\varepsilon_s = 1.0094 + 0.047 \ln(NDVI) \quad (5)$$

where ε_s is the surface emissivity and NDVI is Normalized Difference Vegetation Index. Sensible heat flux (H) is computed in an alternate way in SEBAL. It is called "self calibration" procedure. It was based on the manual identification of wet (well irrigated) and dry (dry ground) pixels in the image. H can be calculated as follows (Bastiaanssen et al., 2005).

$$H = \rho a\ Cp\ T^*\ u^*\ (Wm^{-2}) \quad (6)$$

ρa is density of air ($Kg.m^{-3}$), Cp is Specific heat at constant pressure ($J.\ kg^{-1}.K^{-1}$), T* (K) is the temperature scale and u* ($m.s^{-1}$) the friction velocity. The temperature scale can be formulated as

$$T^* = \Delta T / [\ln(z_2/z_1) - \gamma_h(z_2, L) + \gamma_h(z_1, L)] \quad (K) \tag{7}$$

where ΔT = the vertical air temperature difference between the heights z_1 and z_2; L is the Monin-Obukhov length; and γh is the stability correction for heat transport. Heights z1 and z2 are considered predetermined in SEBAL at 0.1 and 200 m elevation respectively because it is considered that wind speed is spatially constant at height 200 m above the ground. By model inversion method, ΔT, which is required to match between wet and dry pixel under turbulence condition, follows the standard Monin-Obukhov theorem for turbulence exchange processes and thermal convection (Brutsaert 1982). A significant feature of SEBAL is that ΔT or $T(z_1)$-$T(z_2)$ at z_1 and z_2 is determined from hot and cold pixels where H = 0 for wet pixel and H= Rn-G_0 for dry pixels. The friction velocity u* is determined from a single-layer wind speed obtained from the CIMIS weather station. The sensor buried in the soil usually measures the soil heat flux, although the remote sensing of G is possible by taking the daytime ratio of G/Rn with surface temperature (Ts), albedo, and NDVI. Various studies have shown that the soil heat flux can be estimated as a fraction of the net radiation taking into account the albedo, surface temperature, and biomass (Kustas and Daughtry 1990; Kustas et al. 1994a; Bastiaanssen et al 1998; Bastiaanssen 2000). The following equation is derive from Singh et al. (2008)

$$G_0 = [0.3811 \exp(-2.3187NDVI)]Rn \quad (W\ m^{-2}) \tag{8}$$

NDVI is calculated as following:

$$NDVI = (r_{NIR}-r_{red})/(r_{NIR}+r_{red}) \tag{9}$$

where r_{NIR} and r_{red} are the reflectance data of near infrared (band 7) and red (band 5) respectively in MASTER image

The ETa in 24 hours is estimated using instantaneous EF and the daily averaged net radiation R_{n24}. G_0 can be ignored for time scales of 1 day or longer, and net available energy (R_n - G_0) reduces to net radiation (R_n). The daily time scales, ET_{24} (mm/day) can be computed as:

$$ET_{24} = 86400 \times 10^3 \times EF \times R_{n24} / \lambda\rho_w \quad (mm/day) \tag{10}$$

where: R_{n24} (W/m^2) is the 24-h averaged net radiation, λ (J/kg) is the latent heat of vaporization, and ρ_w (kg/m^3) is the density of water, EF is the evaporative fraction.

Program Model and Flowchart

The source code of SEBAL was programmed instead of procuring the original software. It follows the equation given in Bastiaanssen et al. (1995). It follows the energy balance equations given in Bastiaanssen et al. (1995, 1998). The SEBAL model was coded in Interactive Data Language (IDL) programming language incorporated in ENVI 4.0 version with some assumptions going into the model. The model can estimate ET in 90 m ´ 90 m resolution using MASTER data. This program uses imported data from equally-sized images (112 ´ 455 pixels) of 4 blocks of the almond orchards. The flowcharts representing the steps for estimation of ETa are shown in Figure 2. This model inputs MASTER airborne data (ground surface reflectance and temperature) and local weather data (solar radiation and wind speed) to calculate the soil heat flux (G) and sensible heat flux (H). Finally, it outputs the spatial ETa (mm/day).

Input data to the model:

The inputs include wind speed, humidity and solar radiation data at the local weather station and airborne data from MASTER including ground surface reflectance and temperature. The reflectance

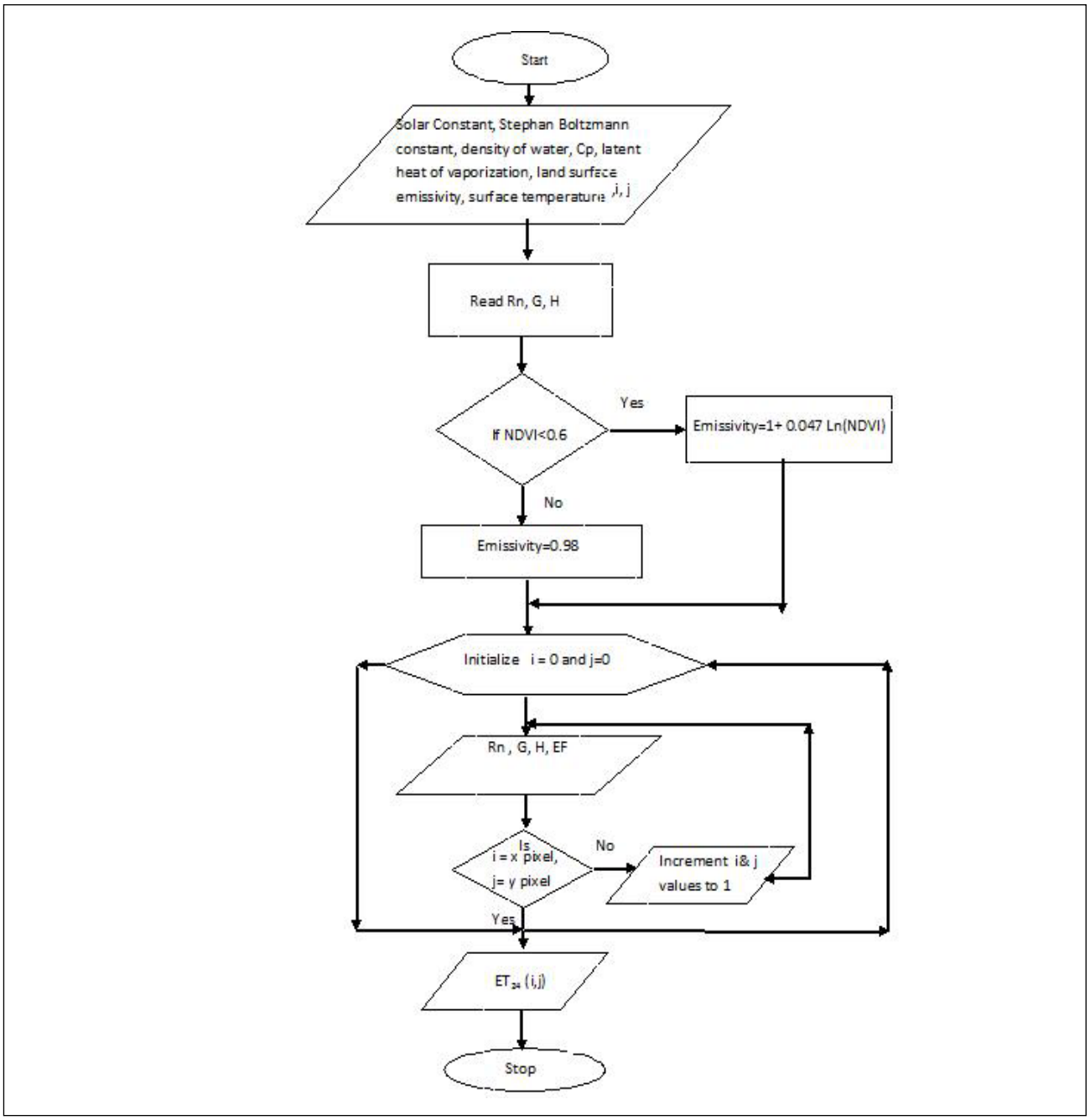

Figure 2. Flow chart representing the steps included in the ENVI+IDL programming for coding SEBAL algorthim in IDL.

has a resolution of 15 m x 15 m for the bands 1 to 3 (Visible and Near-infrared bands) and 30 m x 30 m for the bands 4 to 9 (Shortwave Infrared bands). The temperature data has a resolution 90 m x 90 m. The reflectance data were averaged over 90 m x 90 m to fit the temperature data resolution. This model does not calculate solar radiation, ground surface temperature and reflectances. Instead, the data products are obtained from CIMIS website directly. This simplified the model complexity, which reduce the program work and time.

Output data from the model:

The spatial ETa (mm/day) of almond orchards is the output obtained from the model. The resolution is 30 m x 30 m.

Assumptions in the Model

1. The most major simplification involved prescribing the temperature gradient between 0.1 and 200 meters above the surface to be 1.96 K.

2. The albedo value of almonds obtained from Guo et al., (1995), using spectral data on an airplane flight over California's Central Valley.

3. Evaporative fraction remains constant during daytime.

4. All raster cells/pixels are pure and can be assigned to a unique land cover/use class.

Image Classification and Masking

In supervised classification using Maximum Likelihood classification, the training sites were selected for the region of interest (ROI) of each land cover class. Different ROIs such as almonds, urbans, water soil, pistachios, non-photosynthesis plants and other green vegetations are selected to analyze statistics for classification, masking, and other operations (Figure 3a). Supervised classifications are required to select training areas to define each class. Pixels are compared to the training data. Based on spectral reflectance, they are assigned to the most appropriate class. The statistical characterization of the spectral reflectance for each information class was developed from ENVI image processing software system. Maximum Likelihood Classification is a statistical decision criterion to assist in the classification of overlapping signatures; pixels are assigned to the class of highest probability. After achieving the statistical characterization for each information class, the classification made based on the reflectance of each pixel image, and making a decision about which of the signatures resembles most. The maximum likelihood classifier gave more accurate results than Spectral Angle Mapper; however, it is much slower due to extra computations. Classification accuracy assessment are prepared by selecting testing sites in the image for all the corresponding land cover classes, and confusion matrix was built using ground truth ROIs. A statistical test is performed using the kappa index of agreement for classification accuracy of the image or individual cells (Table 1). Post-processing of classified image was required to estimate accuracy to generalize classes by exporting image-maps and vector GIS. Masking reduces the spatial extent of the analysis by masking out areas of the image, which do not contain data of interest. The almond class map obtained by masking all other land cover classes, which do not have same spectral reflectance characteristics of an almond pixel. This is required for the estimation of evapotranspiration of almond orchards (Figure 3b). Confusion matrix function provided by ENVI, allowed comparison between two classified images (i.e. the classified image and the "truth" image), or a classified image and ROIs. The truth image can be another classified image, or an image created from actual ground based measurements. Since there were no ground reference data for this scene; it was achieved by comparing two of the classifications to each other, and there was comparison between classifications of testing ROIs with training ROIs, although this will not provide an unbiased measure of accuracy (Table 1).

RESULT AND DISCUSSION

ET estimation result

Actual evapotranspiration (ETa) in mm/h for July 24, 2009 was computed by solving the surface energy balance using equations 1, 3, and 6. The spatial variation of ET for the almond class was shown in the Figure 4. It ranges from 0.63 mm/h to 0.70 mm/h for the almond canopy. The average reference evapotranspiration Eto in July 2009 was firstly calculated based on Penmen-Monteith

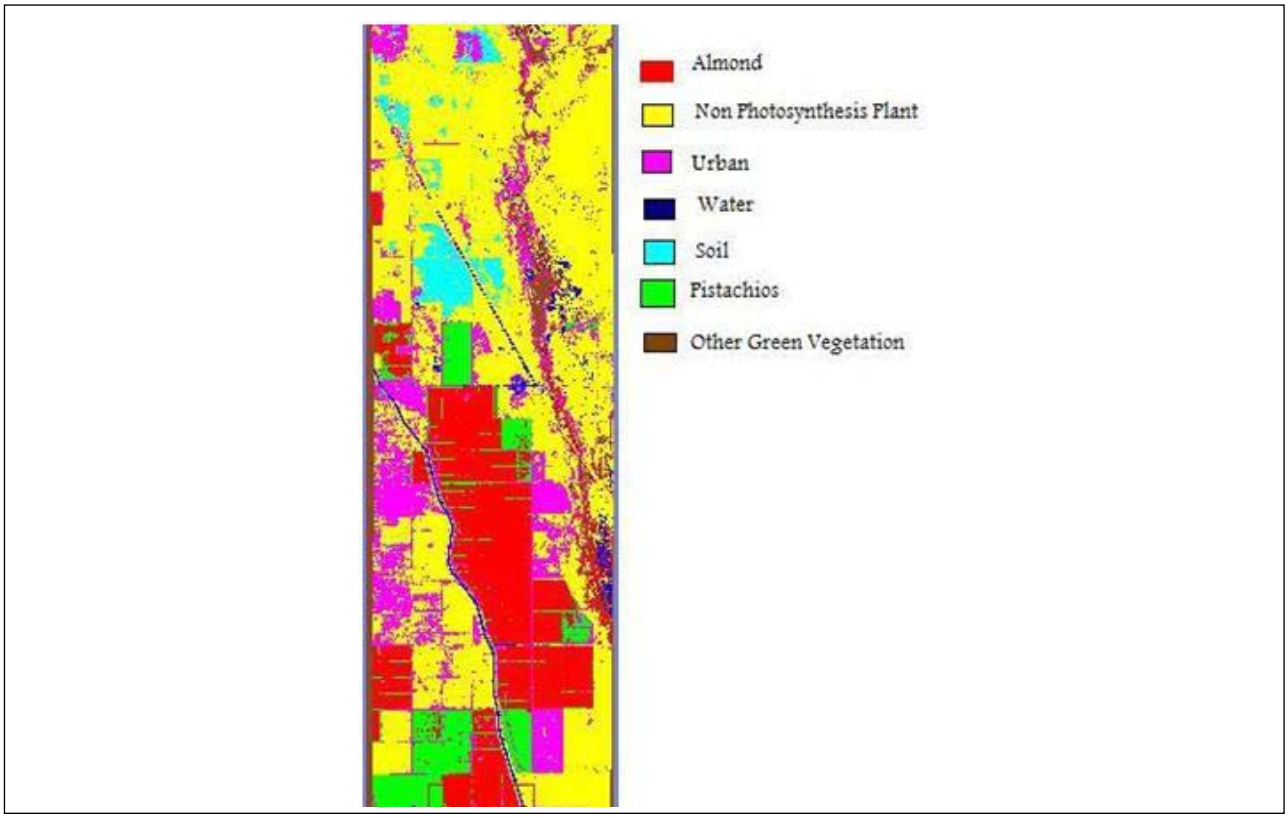

Figure 3a. Supervised classification using maximum likelihood for almond orchards, non-photosynthetic plant (NPV), urban, water, soil, pistachio orchards, and other green vegetations.

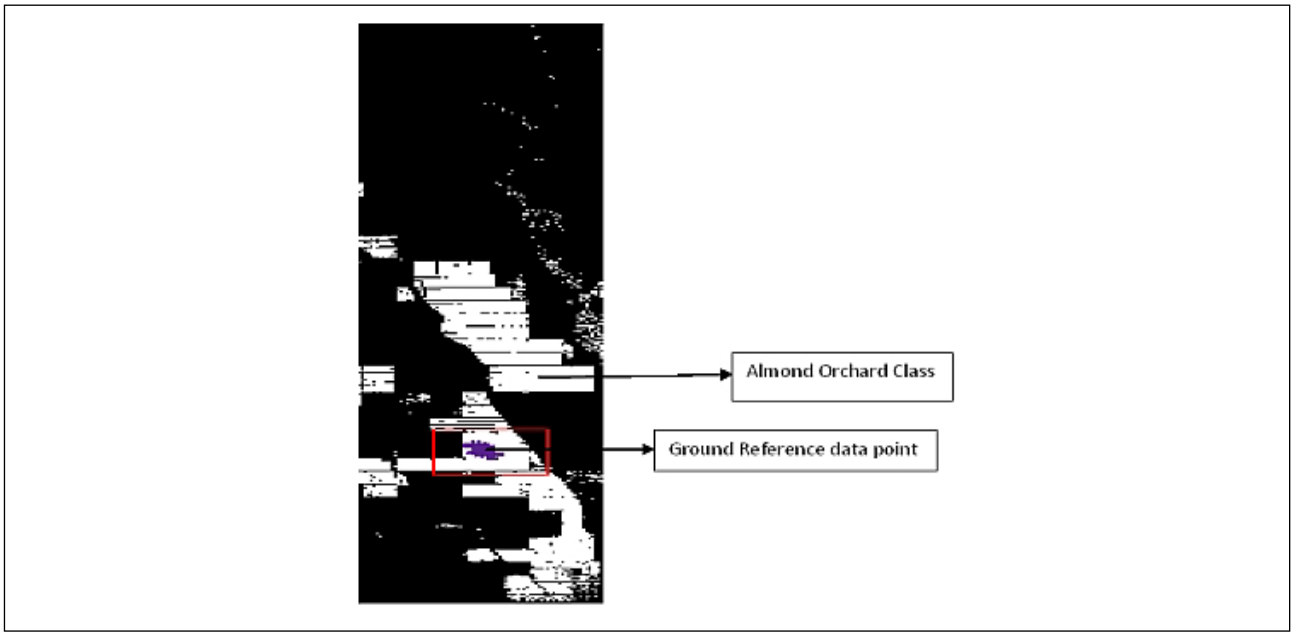

Figure 3b. Post classification: Building Mask. White scale shows the almond class pixel. Other land cover classes are assigned black color using masking technique.

equation as 0.7372 mm/h using CIMIS data. The almond crop coefficient Kc at this time of the year was calculated at 1.05-1.15 in the field. Therefore, the mean empirical estimation of actual evapotranspiration of almond was 0.7519 mm/h. Real time crop evapotranspiration was calculated from the MASTER images. The actual almond evapotranspiration ETa distribution was plotted pixel by pixel in Figure 4.

Table 1. A confusion matrix generated from the classification between training data and testing data.

Classified Category (Training data)	Testing data							Total	User's Accuracy
	Almond	NPV	Urban	Soil	Water	Pistachios	Green Veg		
Almond	387	0	0	0	0	1	0	389	99.49%
NPV	0	252	0	1	1	0	1	253	99.60%
Urban	0	0	69	0	1	1	0	70	98.57%
Soil	0	1	0	221	0	0	0	221	100%
Water	0	0	0	0	267	543	0	267	100.00%
Pistachios	0	0	0	0	0	7	0	543	100%
Green Veg	0	0	0	0	0	0	71	71	100%
Total	387	252	69	222	267	545	72	1814	
Producer's Accuracy	100.00%	100%	100.00%	99.50%	100%	99.63%	98.61%		
Overall accuracy = 99.77 %. Overall Kappa = 0.9973									

Spatial analysis of ETa, NDVI and Ts

Figures 5 and 6 show a positive relationship of evapotranspiration with vegetation indices ($y = 6.055x + 12.663$; $R^2 = 0.9626$), and a negative relationship with land surface temperature ($y = -0.0049x + 2.2212$; $R^2 = 0.8601$) in the study area. This relationship is related to the surface moisture conditions in the arid and semiarid region.

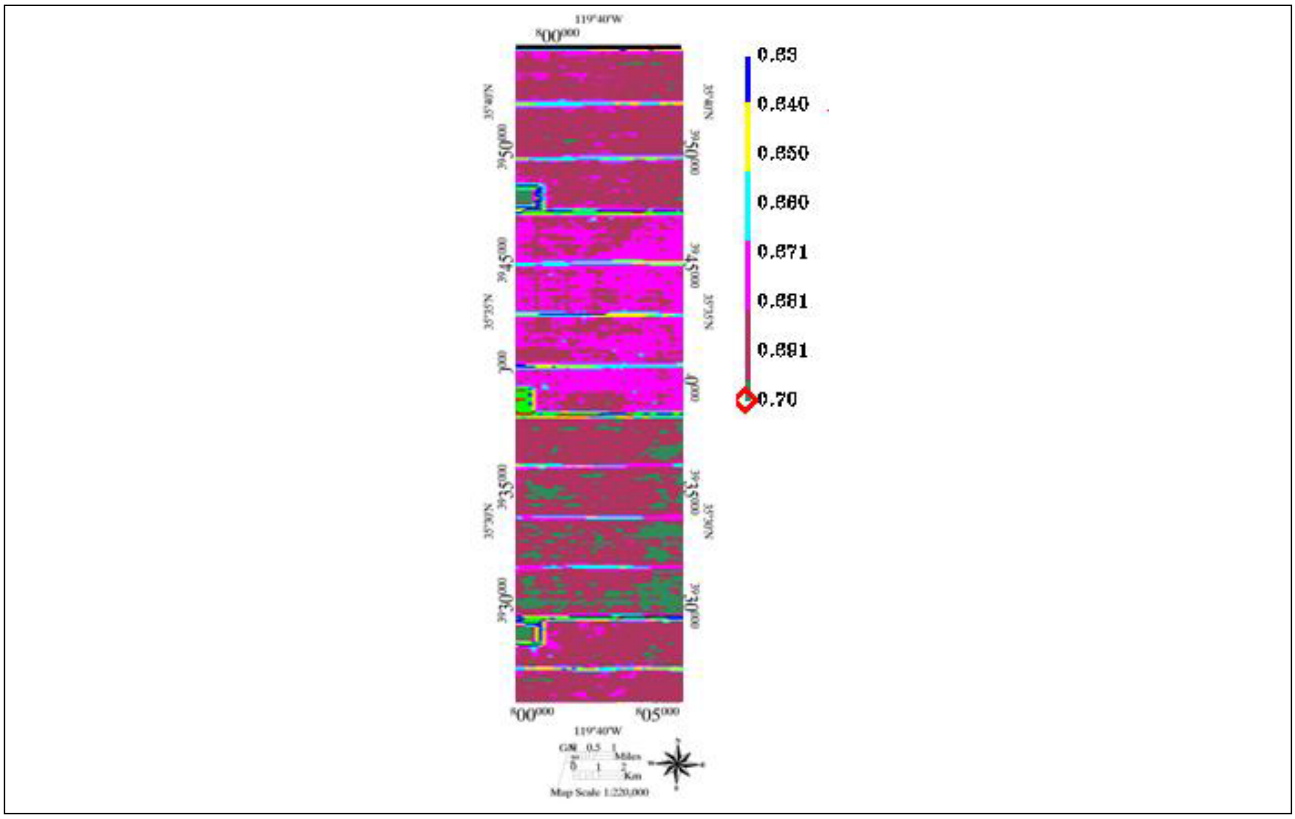

Figure 4. The actual evapotranspiration of almond crop distribution.

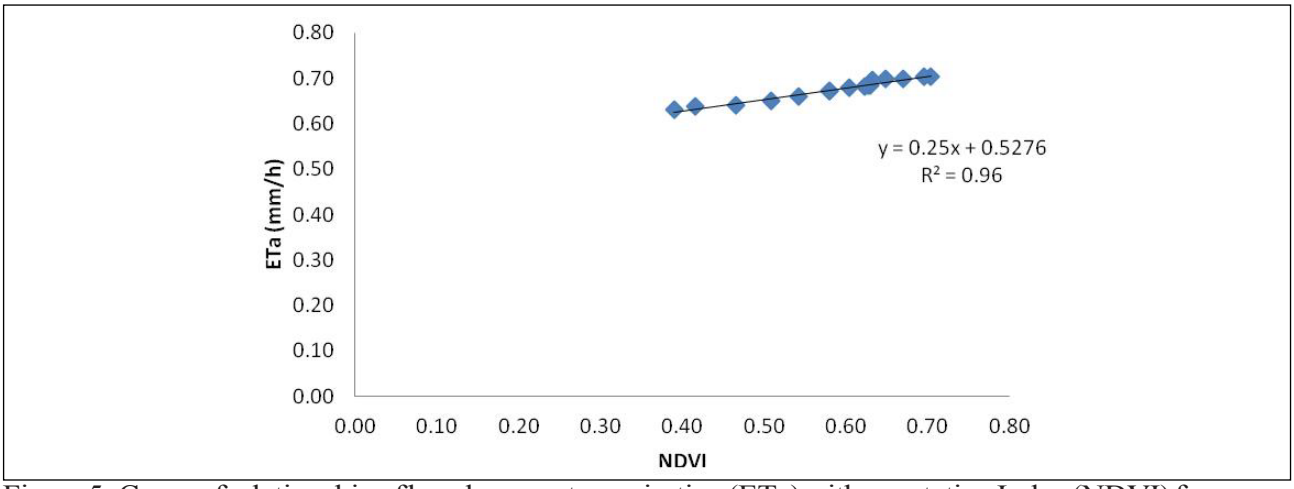

Figure 5. Curve of relationship of hourly evapotranspiration (ETa) with vegetation Index (NDVI) for almond orchards.

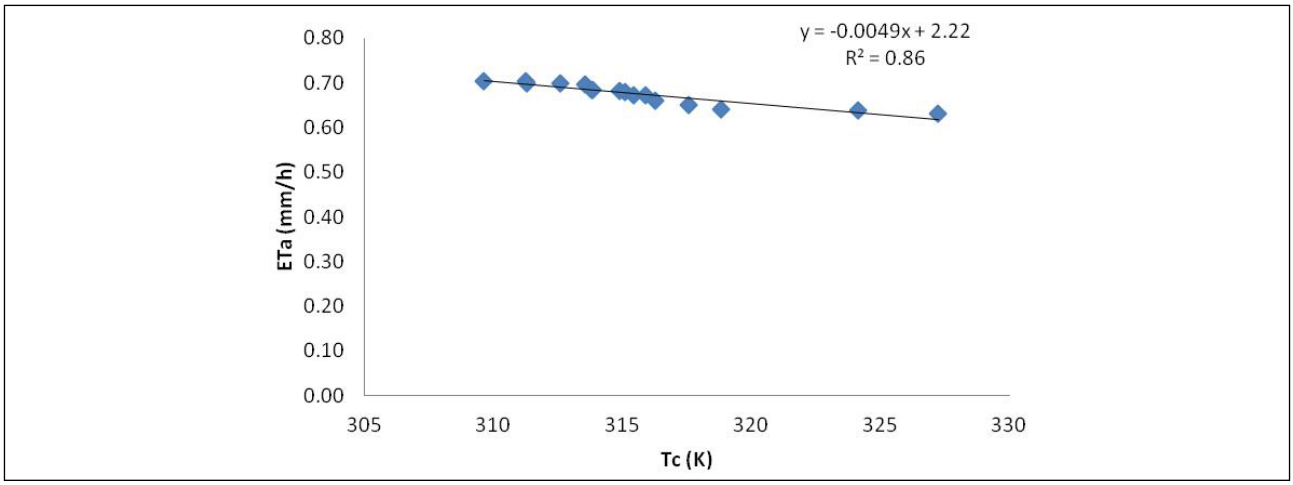

Figure 6. Curve of relationship of hourly evapotranspiration (ETa) with land surface temperature (Tc) for almond orchards.

There is a negative relationship of land surface temperature with vegetation Indices (y = -47.185x + 0.939; R2 =0.9396) in Figure 7. That explains with increase in NDVI, land surface temperature decreases.

Validation of SEBAL with PM models

The validation of these remotely sensed actual ET estimates of almond crop from SEBAL is done by reference ETo obtained from the Penman-Monteith method used by ground measurement by CIMIS. The measured and simulated ET is compared. The relative error (mean percent difference) is calculated as:

Relative Error (%) = (simulation - observation)/observation (11)

The absolute error (mean difference) is calculated as (mm/h):

Absolute Error (mm/h) = (simulation - observation) (12)

The average of daily ETa of remote sensing image is compared with ETa from CIMIS website located at the study area. Figure 8 shows a positive correlation of ETa from Penman-Monteith with SEBAL estimated ETa. The correlation coefficient of ETa estimates from remote sensing with PM

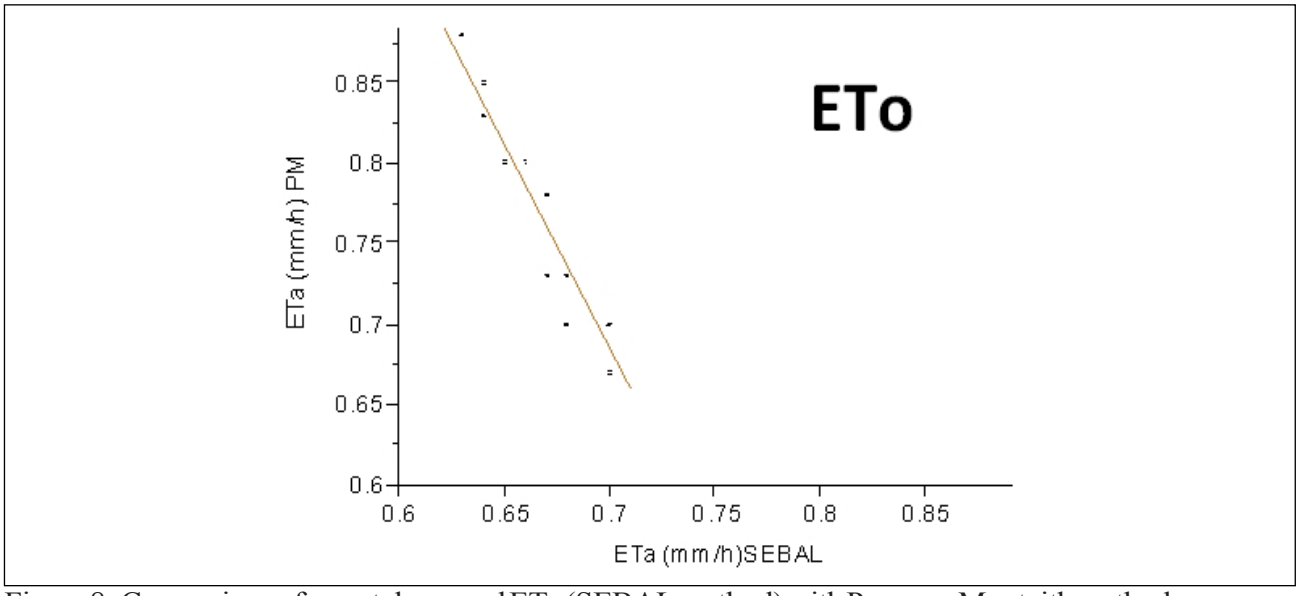

Figure 8. Comparison of remotely sensed ETa (SEBAL method) with Penman-Monteith method ($p<0.0001$).

Table 2. Comparison of actual evapotranspiration of SEBAL approach over Penman-Montieth approach from CIMIS and field data.

ET Estimation Approach (mm/h)	Crop Coefficient	Average actual ET(mm/h)
SEBAL (ETa)	2.29	0.6745
PM-CIMIS (ETa)	1.02	0.7519
Field (ETa)	1.15	1.26

was 0.93. The mean difference between actual ETa from SEBAL in almond and Penman-Monteith for over all observations associated with ETa was 0.77 mm/h. Table 2 compares ET between the field data used by CIMIS and remote sensing method. The mean percent difference for ETa from SEBAL and CIMIS Penman-Monteith (PM) is calculated as (PM - SEBAL) / SEBAL was 0.109%.

CONCLUSION

Cloud free aerial MASTER image obtained during the almond pre-harvesting season on July 24, 2009 was processed for Paramount farm in California using a remote sensing based SEBAL model. The modified SEBAL is capable of computing the spatial almond hourly water use with resolution of 30 m x 30 m. The average actual evapotranspiration (ETa) estimated from SEBAL is 0.67 mm/h. The simulated ETa was compared with that from ground measured PM method. The mean percent difference (relative error) was 0.10% and the mean difference (absolute error) was 0.77 mm/h.

The result shows a positive relationship of ETa with vegetation indices ($y = 0.25x + 0.52$; $R^2 = 0.96$), and a negative relationship of ETa with canopy temperature ($y = -0.0049x + 2.22$; $R^2 = 0.86$) in the study area. This relationship is related to the surface moisture conditions in the arid and semiarid region. There is a negative relationship of canopy temperature with vegetation Indices ($y = -47.1x + 343.17$; $R^2 = 0.93$) which explains with increase in NDVI, the canopy temperature decreases.

ACKNOWLEDGMENT

We are thankful to the NASA Student Airborne Research Program 2009, National Suborbital Education and Research Center (NSERC) of the University of North Dakota. In addition, we would like to thank the MASTER teams from NASA AMES, Paramount Farms for the use of their facilities, the CSTARS field team from UCD, and Blake Sanden from the UCD agriculture extension for coordination, data exchanges and fieldwork. This paper was reviewed by Dr. Seth Xeflide of the Department of Land Sciences, at Old College, Canada and by Dr. Brijesh Kumar Yadav of the Department of Water Resources Engineering at Indian Institute of Technology, New Delhi, India. We are grateful for their reviews.

REFERENCES

Allen, R.G., L.S. Pereira, D. Raes, and M. Smith. 1998. Crop Evapotranspiration. Irrigation and Drainage. Food and Agriculture Organization of the United Nations. Rome, Italy, pp. 56.

Bastiaanssen, W.G.M., M. Menemti, R.A. Feddes, and A.A.M Holtslag. 1998. A Remote Sensing Surface Energy Balance Algorithm for Land (SEBAL). Part 1: Formulation, Journal of Hydrology, Vol. 212/213, pp. 198-212.

Bastiaanssen, W.G.M., D.J. Molden, and I.W. Makin, 2000. Remote sensing for irrigated agriculture: examples from research of possible applications, Agricultural Water Management, Vol. 46(2), pp. 137-155.

Bastiaanssen, W. G. M. 2000. SEBAL based sensible and latent heat fluxes in the irrigated Gediz Basin, Turkey. J. Hydrol., Vol. 229, pp. 87–100.

Bastiaanssen, W.G.M., E.J.M. Noordman, H. Pelgrum, G. Davids, and R.G. Allen, 2005. SEBAL for spatially distributed ET under actual management and growing conditions, Journal of Irrigation and Drainage Engineering, Vol. 131(1), pp. 85-93.

Bastiaanssen W. G. M., E. J. M. Noordman; H. Pelgrum; G. Davids, B., P. Thoreson, and R.G. Allen. 2005. SEBAL Model with Remotely Sensed Data to Improve Water-Resources Management under Actual Field Conditions. Journal of Irrigation and Drainage Engineering, Vol. 131, pp. 85-93.

Brutsaert, W. 1982. Evaporation into the Atmosphere. Reidel, Dordrecht, The Netherlands

California Dept. of Food and Agriculture. 2009. http://www.cdfa.ca.gov/egov/Press_Releases/Press_Release.asp?PRnum=09-009, California Department of Water Resources Revised June 18, 2009.

Courault, D., B. Seguin, and A. Olioso. 2003. Review to estimate evapotranspiration from remote sensing data: some examples from the simplified relationship to the use of mesoscale atmospheric models. ICID workshop on remote sensing of ET for large regions, 17th September, 2003.

"Drought: A Paleo Perspective – 20th Century Drought". National Climatic Data Center. http://www.ncdc.noaa.gov/paleo/drought/drght_history.html.

Davis, G.H., J.H. Green, F.H. Olmsted, and D.W. Brown. 1959. Ground-water conditions and storage capacity in the San Joaquin Valley, California: U.S. Geological Survey Water-Supply, Vol. 1469, pp. 287.

Daughtry, C.S.T., W.P. Kustas, M.S. Moran, P.J. Pinter, R.D. Jackson, P.W. Brown, W.D. Nichols, and L.W. Gay. 1990. Spectral estimates of net radiation and soil heat flux. Remote Sens. Environ., Vol. 32, pp. 111–124.

Engman, E.T., and R.J. Gurney. 1991. Remote sensing in hydrology, Chapman and Hall, London.

Kustas, W.P., and C.S.T. Daughtry. 1990. Estimation of the soil heat flux/net radiation ratio from spectral data. Agricultural and Forest Meteorology, Vol. 49, pp. 205-223.

Kustas, W.P., E.M. Perry, P.C. Doraiswamy, and M.S. Moran. 1994a. Using satellite remote sensing to extrapolate évapotranspiration estimates in time and space over a semiarid rangeland basin. Remote Sens. Environ, Vol. 49, pp. 275-286.

Kustas, W.P., M.S. Moran, K.S. Humes, D.I. Stannard, P.J. Pinter, L.E. Hipps, E. Swiatek, and D.C. Goodrich. 1994a. Surface energy balance estimates at local and regional scales using optical remote sensing from an

aircraft platform and atmospheric data collected over semiarid rangelands. Water Resour. Res., Vol. 30(5), pp 1241–1259.

Kustas, W.P., and J.M. Norman. 1996, Use of remote sensing for Evapotraspiration monitoring over land surfaces IAHS Hydrological Science Journal, Vol. 41, pp 496-526.

Kustas, W.P., M.C. Anderson, J.N. Norman, and A.N. French. 2003. Estimating subpixel surface temperatures and energy fluxes from the vegetation index-radiometric temperature relationship. Remote Sensing of Environment, Vol. 85, pp. 429-440.

Hook, S.J., J.J. Myers, K.J. Thome, M. Fitzgerald, and A.B. Kahle. 2001. The MODIS/ASTER airborne simulator (MASTER) a new instrument for earth science studies, Remote Sensing of environment, Vol. 76, pp. 93-102

Singh, R.K., A. Irmak, S. Imrak, and D. L . Martin. 2008. Application of SEBAL Model for Mapping Evapotranspiration and Estimating Surface Energy Fluxes in South-Central Nebraska. Journal of Irrigation and Drainage Engineering, Vol. 134(6), pp. 722-729.

ADDRESS FOR CORRESPONDENCE
Sagarika Roy
Montclair State University
1 Normal Ave, Upper Montclair
New Jersey 07043
Email: roys2@mail.montclair.edu